

**Two-phase modelling of the rings in the RXTE two-color diagram
of GRS 1915+105**

Osmi Vilhu

Observatory, Box 14, FIN-00014 University of Helsinki, Finland

and

Jukka Nevalainen

Harvard-Smithsonian Center for Astrophysics, 60 Garden Street, Cambridge, MA 01238,
USA, and Observatory, University of Helsinki, Finland

Received ;; accepted :

ABSTRACT

The Galactic superluminal source GRS 1915+105 was found to experience a peculiar X-ray variability in a narrow count rate range (9300 - 12100 cts/s, 5 PCU's) of the Proportional Counter Array (PCA) onboard the Rossi X-ray Timing Explorer (RXTE). This can be seen as a ring-shaped pattern in the two-color diagram of count rates, where the hard hardness $F(13-40\text{keV})/F(2-13\text{keV})$ is plotted against the soft hardness $F(5-13\text{keV})/F(2-5\text{keV})$. The system runs one cycle with periods ranging between 50 - 100 s for different observations, one rotation in the 2-color diagram corresponding to the time between two contiguous maxima in the light curve. We model this behaviour successfully with the help of a self-consistent 2-phase thermal model where seed photons from an optically thick classical disk are Comptonized in a hot spherical corona surrounding the inner disk (Poutanen and Svensson (1996), Vilhu et al. (1997), Nevalainen et al. (1998)). In the model, changes of two parameters regulate the paths in the 2-color diagram: the black body temperature T_{in} of the inner disk and the Thomson optical depth multiplied by the electron temperature of the hot phase τT_e . These parameters oscillate with time but with a phase-shift between each other, causing the ring-shaped pattern. During the observation studied in more detail (20402-01-30-00), the inner disk radius varied with 97 s period between 20 - 35 km with an anticorrelation between the coronal τT_e and the mass accretion rate \dot{M} through the disk, possibly indicating a coupling between the disk and coronal accretion. During a typical cycle, the inner disk radius rapidly shrank and returned more slowly back to the original larger value. In the rings we may see phenomena close to the black hole horizon under near Eddington accretion rates.

Subject headings: accretion, accretion disks—binaries:close—black hole
physics— instabilities—X-rays:stars—stars:individual:GRS 1915+105

1. Introduction

The X-ray transient GRS 1915+105 was discovered by Castro-Tirado et al. (1992). Mirabel et al. (1994) found superluminal jets at an angle of 70° to the line of sight in this Galactic black hole candidate which lies at a kinematic distance of 12.5 ± 1.5 kpc (Chaty et al. 1996). The Rossi X-ray Timing Explorer has been monitoring it frequently, making the data openly available to the scientific community. In this way GRS 1915+105 has become an important target for studying accretion phenomena close to a potential black hole.

A rich pattern of variability has already emerged from the RXTE data (Greiner et al. (1996), Morgan et al. (1997), Chen et al. (1997), Taam et al. (1997), Belloni et al. (1997a), Belloni et al. (1997b), Markwardt (1997)). In particular, Belloni et al. (1997b) interpreted the variability during their observations (mean 5 PCU count rate 14000 cts/s) as a rapid disappearance of the inner disk (through the horizon), and suggested that the viscous time scale controls the variability in this radiation-pressure dominated region . They modelled the spectra in the 2 - 40 keV range with the classical multi-temperature disk with a power-law component. This modelling allowed the study of the changes of the inner disk radius which, during the observations, varied between 20 - 80 km.

In the present letter we report a variability of GRS 1915+105 which manifests itself as a ring-shape pattern in the 2-color diagram. Further, we model this behavior with the help of a self-consistent two-phase model where seed photons from a classical disk are Comptonized in a spherical corona surrounding the inner disk.

2. Observations

We collected several Proportional Counter Array (PCA) observations from the TOO-archive of RXTE, with typical durations of a few hours. The Standard 2 data

with 128 channels of spectral information and 16-sec temporal resolution were used. The background was subtracted although its effect was not crucial (being around 10 per cent in the HR2-color). The data were binned into 16 sec time-bins and further (following Belloni et al. (1997b)) into two X-ray colors $HR1 = B/A$ and $HR2 = C/(A + B)$, where A, B and C are the counts in the 2.0 - 5.0 keV (channels 3-10), 5.0 - 13.0 keV (channels 11-32) and 13.0 - 40.0 keV (channels 33-77) intervals, respectively. Color-color diagrams were constructed showing many different patterns with a strong dependence on the average count-rate.

Particularly interesting features were the **rings**, occurring at the rising phase of the RXTE/ASM light curve (see Fig.1 and Table 1) and having mean PCA count rates in a narrow interval 9300 - 12100 cts/s (2 - 40 keV, 5 PCU's). These are discussed in the next Chapter. They form a sub-class of the quasi-periodic structure in the time domain, discussed earlier in the references cited above and showing hysteresis behavior and closed loops in the 2-color diagram. We call them as 'rings', separating them from the other observations, due to their rather regular and ring-shaped paths in the 2-color diagram. For comparison, the 2-color diagram of the observation analysed by Belloni et al. (1997b) looks like a crescent.

EDITOR: PLACE TABLE 1 HERE.

EDITOR: PLACE FIGURE 1 HERE.

3. Rings in the X-ray 2-color diagram and their modelling

Table 1 and Figure 2 summarize the seven observations showing ring-behavior. For comparison, the observation analyzed by Belloni et al. (1997b), and one observation in the long quiescent lull-phase, are indicated (see the dotted lines in Fig.1).

EDITOR: PLACE FIGURE 2 HERE.

EDITOR: PLACE FIGURE 3 HERE.

EDITOR: PLACE FIGURE 4 HERE.

The system runs clock-wise in the 2-color diagram with average periods between 47 - 97 s (see Table 1), computed as the total observing time divided by the number of maxima in the light curve. This number of maxima equals to the number of rotations in the 2-color diagram, since one rotation corresponds to the time between two contiguous maxima. Timing work with better time resolution is in progress, in the present letter we concentrate on average (over 16 s) behavior of the oscillations.

Figures 3 and 4 give more details of one particular observation (20402-01-30-00) and its time evolution. This observation was selected due to its long period (97 sec), allowing to construct reasonably accurate light curves despite the 16-s time resolution. The fastest speed (angular velocity) along the ring of this particular observation was on the average 80 degrees/16 sec (as seen from the center of the ring). The 16 sec averaging should be statistically adequate to characterise the ring when many data-points from different phases are collected.

We attempted to model the rings for this letter. A more detailed spectral fitting will be presented in a forthcoming paper, including simultaneous HEXTE and time-averaged BATSE data. The simplest way would be to use the multi-color disk black body model with a power-law component, as done in some of the papers cited above. However, the power-law component alone includes no physics nor system geometry, although a popular explanation for its origin is the Comptonization process.

Instead, we used a two-phase thermal radiative model to couple the disk and Comptonized radiation. In the model, the cool phase consists of an optically thick multi-temperature disk, generating the observed soft spectrum and serving as a source of the seed photons Comptonized in the spherical hot phase (corona) surrounding the inner disk (giving rise to the power-law component). The geometry resembles and approximates that of the advective disks as developed e.g. in Esin et al. (1997). The radiative transfer was handled by the iterative scattering method (ISM) developed by Poutanen and Svensson (1996) and incorporated into the XSPEC spectral fitting software of the XANADU package (for more details of the model, see Vilhu et al. (1997), Nevalainen et al. (1998)). In a specific geometry (a fixed ratio of the inner disk and coronal radii, = 0.5 used here) the model is self-consistent and predicts the normalization between the soft and power-law components, as well as the power-law photon index.

The free model parameters are the black body temperature T_{in} at the inner disk (with the temperature-stratification in the disk as $T(r) = T_{in}(r/R_{in})^{-3/4}$), the electron temperature T_e and the Thomson optical depth τ of the hot corona. The inclination was fixed to 70° (Mirabel et al. (1994)), assuming that the jets are perpendicular to the disk. Information of the high energy cut-off is needed to fix the coronal temperature which is possibly beyond the RXTE capability (in a forthcoming paper we try to fix it with the HEXTE data). In the narrow PCA energy interval 2-50 keV, τ and T_e cannot be separated but their product τT_e uniquely specifies the spectrum together with T_{in} . The Hydrogen column was fixed at $N_H = 4.5 \cdot 10^{22} \text{ cm}^{-2}$ as in Belloni et al. (1997b). This value was adopted since it is close to our preliminary fits. By changing the value, one shifts the model curves of Fig.3 in the North-East - South-West direction. Using $N_H = 3.5 \cdot 10^{22} \text{ cm}^{-2}$ gives 1.4 and 1.2 times larger T_{in} and τ values, respectively, having no qualitative effect on our conclusions. Just the parameter values would be somewhat different.

The curves added to Fig.3 show the above reference model as a function of T_{in} and $\tau_{50} = \tau T_e / 50 \text{keV}$. The effects of these two parameters act in the 2-color diagram perpendicularly to each other. The cycling behavior can be understood as a variability of these two parameters with a phase shift (the maxima or minima do not coincide in time). The model gives the disk luminosity (proportional to $R_{in}^2 T_{in}^4$) from which the inner disk radius R_{in} can be computed (assuming $d = 12.5 \text{ kpc}$). The light curves of the observation 20402-01-30-00 are shown in Fig.4, as interpolated from the reference model curves in Fig.3.

4. Discussion

We have analysed the data using the 16 s time resolution of Standard 2 data. Hence, any existing sub-structure (like in the observation by Taam et al. (1997) was smoothed out. However, the time resolution used is sufficient to demonstrate the qualitative nature and shape our ring-data in the 2-color diagram (see Figures 2 and 3) and the applicability of our modelling at this resolution. Further work is clearly needed for a more detailed timing and spectral analysis of the observations in Table 1.

The changes of T_{in} and $\tau_{50} = \tau T_e / 50 \text{keV}$ in our modelling are sufficient to explain the whole pattern of different paths in the 2-color diagram. The ratio of the soft and hard luminosities, the power-law photon index α and τ_{50} are strongly correlated (for small values of τ and T_e , the Kompaneets y -parameter is close to their product). The spectrum in the PCA energy-interval is determined by T_{in} and τ_{50} , and α is uniquely determined by τ_{50} (e.g. $\alpha = 3.2$ and 2.5 when $\tau_{50} = 0.5$ and 1.0 , respectively). To check the consistency we run the observations analyzed by Belloni et al. (1997a) through our models in the 2-color diagram. This resulted in a qualitatively similar photon index behavior as a function of time to that which was obtained with the diskbb + power-law modelling. Preliminary studies of individual ring-spectra (accumulated by count rate criteria) also confirm our

modelling but these will be the topics of a separate paper.

The variability is probably controlled by the viscous time scale as demonstrated for one set of observations by Belloni et al. (1997b), although it remains to be studied whether this is the case for all observations, in particular for the rings discussed in the present paper.

The mass accretion rate (through the disk) can be computed from the formula of classical viscous disks (Frank et al. (1992)): $\dot{M} = 8\pi R_{in}^3 \sigma T_{in}^4 / 3GM$. The rates computed from this formula are high and the inner disk lies inside the unstable radiation-dominated region of the thermal balance curve. Because of this, the disk is probably advection dominated and the mass transfer rates computed may be in error. Further, at very high rates the accretion through the disk and corona may anticorrelate (Esin et al. (1997), their Sec.3.4) and the true accretion rate might behave quite differently from that computed from the above formula.

To obtain a better idea of what is happening, mean light curves of important parameters were accumulated along the ring-path of Fig.3 (see Fig.5).

EDITOR: PLACE FIGURE 5 HERE.

The whole ring-cycle can be visualized in the following way (see Fig.5):

Locally the inner disk is unstable, perhaps because it is inside the radiation pressure dominated zone. The mass transfer rate \dot{M} starts to increase from its value $0.15\dot{M}_{Edd}$ (of $10M_{\odot}$ using the classical formula above and $\dot{M}_{Edd} = L_{Edd}/c^2$) leading to slow increases of the luminosity and the inner disk radius. At a certain point the inner disk starts to shrink rapidly, leading to the count rate spike and a clear minimum of the coronal τ_{50} . At the same time \dot{M} reaches its maximum $0.5\dot{M}_{Edd}$ and returns rapidly to its smaller original value. After the minimum radius has been reached the mass transfer rate starts to increase again and a new cycle starts.

τ_{50} and \dot{M} were determined quite independently, so their anticorrelation in Fig.5 is remarkable. This might indicate that a fraction of the mass accretion is channelled through the disk, and another fraction through the corona (reflecting its optical depth τ_{50}). During the whole process the total accretion may remain constant, just its different contributions vary.

We note that during each individual cycle, the system spends half of its time in the lower-right corner of Fig. 3 (a state of minimum count rate), and only rapidly visits the state of high count rates. The rising times are also longer than the decay times. Sometimes, but not always, the system seems to spend additional time during count rate and R_{in} maxima. This time-asymmetry may give some additional information for the reason of the peculiar behavior of the system. The picture of a rapid disappearance of the whole inner disk annulus through the horizon (as in the Belloni et al. (1997b) case) is not so simple here, since the emptying process (the time evolution of increasing R_{in}) is slow (see Fig.5). Of course, after the rapid shrinking phase, some part of the inner disk could have disappeared (note in Fig.5, the perhaps not so significant short rise after the minimum).

The main difference between the rings discussed here and the observations analyzed by Belloni et al. (1997b) is that in the latter case the amplitudes of T_{in} and τ_{50} are in phase (the minima of τ_{50} correspond to the maxima of the count rate and T_{in}). For the rings, instead, there is a phase shift between these two parameters. This follows simply by converting (at each time bin) the observed pairs of (HR1,HR2)-values into the corresponding pairs of (T_{in} , τ_{50})-values, using the theoretical grid shown in Fig.3. In the Belloni et al. (1997b) observations, T_{in} maxima and τ_{50} minima coincide (with no phase-shifts), following from the crescent-like form of the 2-color diagram (see the dots in Fig.2). Future work on disk instabilities should explain the physical reasons of these different paths.

Further, the mean count rate, the mean inner disk radius and its amplitude were larger

in the Belloni et al. (1997b) case. Hence, the ring-behavior might be characteristic to disk instabilities very close to the innermost stable Keplerian orbit, where the relativistic potential barrier is small and just a small change in angular momentum leads to accretion through the horizon (Frank et al. (1992)). However, the minimum values of R_{in} obtained (20 km) are too small for a non-rotating black hole and require a rotating Kerr hole to be related to the innermost stable orbit, unless the central mass is smaller than 2-3 solar masses.

5. Conclusions

We found a peculiar form of variability (**rings**) of GRS 1915+105 in the RXTE/PCA 2-color diagram (see Table 1 and the Figures 2 and 3). This pattern was observed in a narrow interval 9300 - 12100 cts/s (2 - 40 keV, 5 PCU's), intermediate between the very high and lull states (see Fig.1). The mean period of variability is between 50 - 100 sec. There is no direct correlation between the cycle-period and count rate, although a real variability (spin-ups and spin-downs) may have taken place. The system spent most of the time in the low count rate level and only rapidly visited the state of high count rates (with longer rise than decay times).

We modelled this behavior with a 2-phase self-consistent radiative thermal model where an optically thick multi-temperature disk gives rise to the soft part of spectrum and serves as a source of seed photons, Comptonized in the hot spherical corona surrounding the inner disk. We explain the variability with the help of two parameters (T_{in} and $\tau_{50} = \tau T_e/50\text{keV}$), and with a phase-shift between their light curve amplitudes.

During the observation studied in more detail (20402-01-30-00), the inner disk radius R_{in} oscillated between 20 - 35 km, the smallest value was reached somewhat after the count

rate maximum and τ_{50} -minimum. During a typical cycle, the inner disk radius shrinks, after which returned more slowly back to the original larger value (see Fig.5). \dot{M} and τ_{50} anticorrelated, possibly indicating a balance between the accretion flows through the disk and corona (in the sense that the total accretion rate might remain constant). In the rings we may see interesting phenomena very close to the black hole horizon during high accretion rates.

We are grateful to the whole staff of the RXTE Guest Observer Facility at GSFC, especially to Tess Jaffe, Gail Rohrbach and Padi Boyd, for the great and friendly assistance during our stay at GOF. We thank Craig Markwardt for discussions of his interesting results, Juri Poutanen for his ISM models and most valuable help and advice during their usage and interpretation of the results, and Diana Hannikainen for reading the manuscript and for comments. We also thank the referee for useful criticism. JN thanks the Harvard Smithsonian Center for Astrophysics for hospitality and the Smithsonian Institute for a Predoctoral Fellowship and the Academy of Finland for a supplementary grant.

Table 1. RXTE/PCA ring-data.

ID	JD - 2450000	5 PCU cts/s	cycle time (sec)
20402-01-30-00	595.035	9260	97
20402-01-31-00	603.083	10300	74
20402-01-31-01	604.986	10420	49
20402-01-31-02	605.135	10540	47
20402-01-32-01	608.847	11320	67
20402-01-32-00	608.985	11300	82
20402-01-34-01	622.333	12150	53

REFERENCES

- Belloni, T., Mendez, M., King, A.R., van der Klis, M., and van Paradijs, J. 1997, ApJ, 479, L145.
- Belloni, T., Mendez, M., King, A.R., van der Klis, M., and van Paradijs, J. 1997, ApJ, 488, L109.
- Castro-Tirado, A.J., Brandt, S., and Lund, N. 1992, IAU Circ. 5590
- Chaty, S., Mirabel, I.F., Duc, P.A., Wink, J.E., and Rodriguez, L.F. 1996, Astron.Astrophys., 310, 825.
- Chen, X., Swank, J.H., and Taam, R.E. 1997, ApJ, 477, L41
- Esin, A.A., McClintock, J.E., and Narayan, R. 1997, ApJ, 489, 865
- Frank, J., King, A., and Raine, D. 1992, Accretion Power in Astrophysics, 2nd Ed., Cambridge Univ. Press.
- Greiner, J., Morgan, E., and Remillard, R.A. 1996, ApJ, 473, L107
- Markwardt, M., 1997 private comm.
- Mirabel, I.F. and Rodriguez, L.F. 1994, Nature, 371, 46
- Morgan, E., Remillard, R.A., and Greiner, J. 1997, ApJ, 482, 993
- Nevalainen, J., Vilhu, O., Poutanen, J., Gilfanov, M. and Vargas, M. 1998, in N.J.Westergaard, O.Vilhu and R.Svensson (eds.), 'Nordic Conference in Theoretical High Energy Astrophysics', Physica Scripta (in press)
- Poutanen, J. and Svensson, R. 1996, ApJ, 470, 249
- Taam, R.E., Chen, X., and Swank, J.H. 1997, ApJ, 485, L83

Vilhu, O., Nevalainen, J., Poutanen, J., Gilfanov, M., Durouchoux, Ph., Vargas, M., Narayan, R. and Esin, A. 1997, in Charles D. Dermer, Mark S. Strickman and James D. Kurfess (eds.), Proceedings of the Fourth Compton Symposium, AIP Conference Proceedings 410, p.887.

Fig. 1.— The ASM light curve (2 - 13 keV) of GRS 1915+105 with the ring-observations of Table 1 marked with vertical dashed lines. The dotted lines show the times of other observations discussed in the text (and marked in Fig.2).

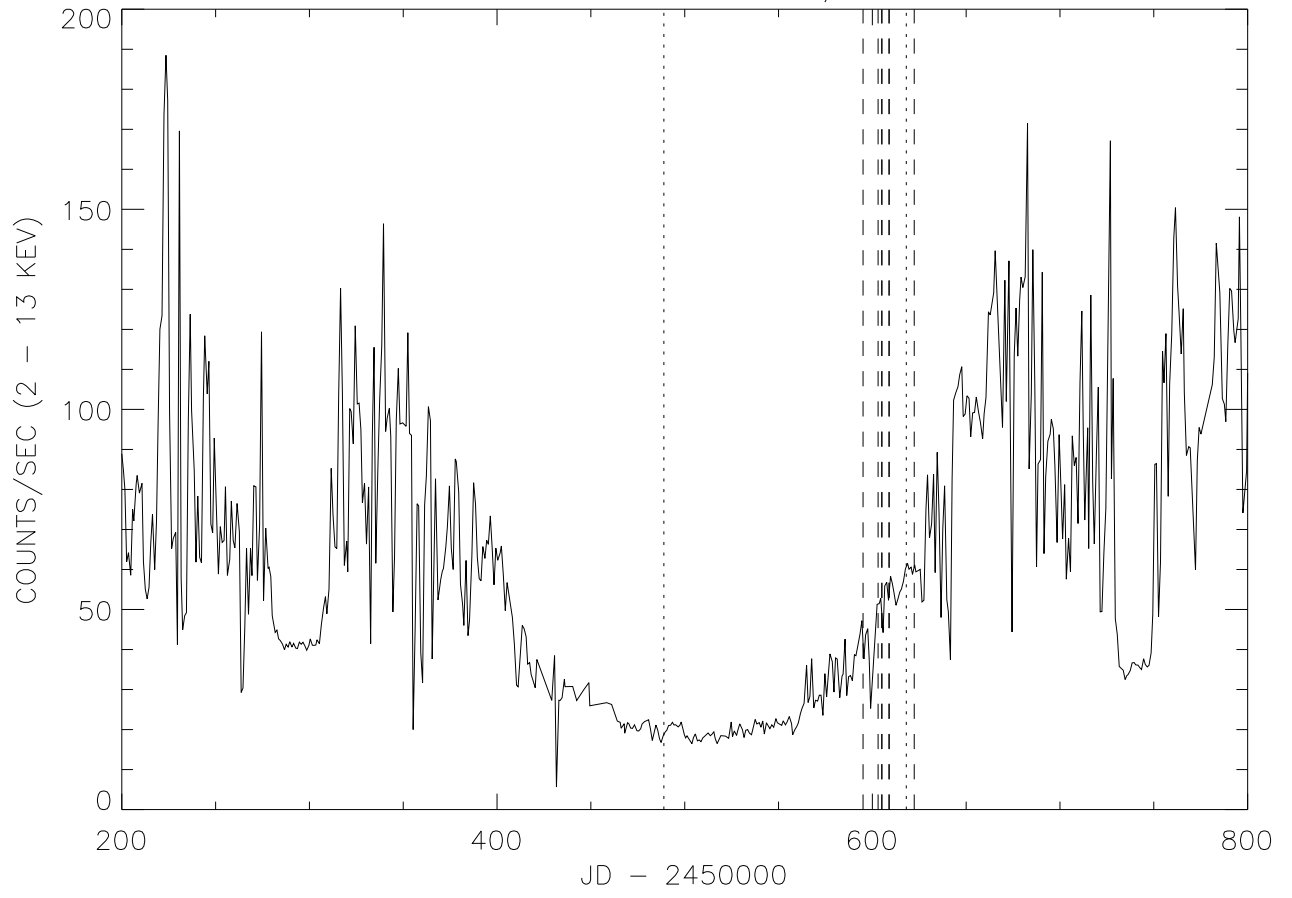
Fig. 2.— The ring-data of Table 1 plotted in the 2-color diagram with 16 s time-binning (plus-signs). For comparison, the observation analyzed by Belloni et al. (1997b) (marked with points) and one observation from the long lull-phase of Fig.1 (the small patch at the upper-right marked with diamonds) are overplotted.

Fig. 3.— The observation 20402-01-30-00 (see Table 1) plotted in the 2-color diagram with 16 sec time-binning (neighboring data-points in the light curve joined with lines). The big arrows show the clock-wise evolution with 97 s mean cycle period. Positions of maximum and minimum values of some variables are marked. The 2-phase model curves (see the text) are overplotted with dotted lines.

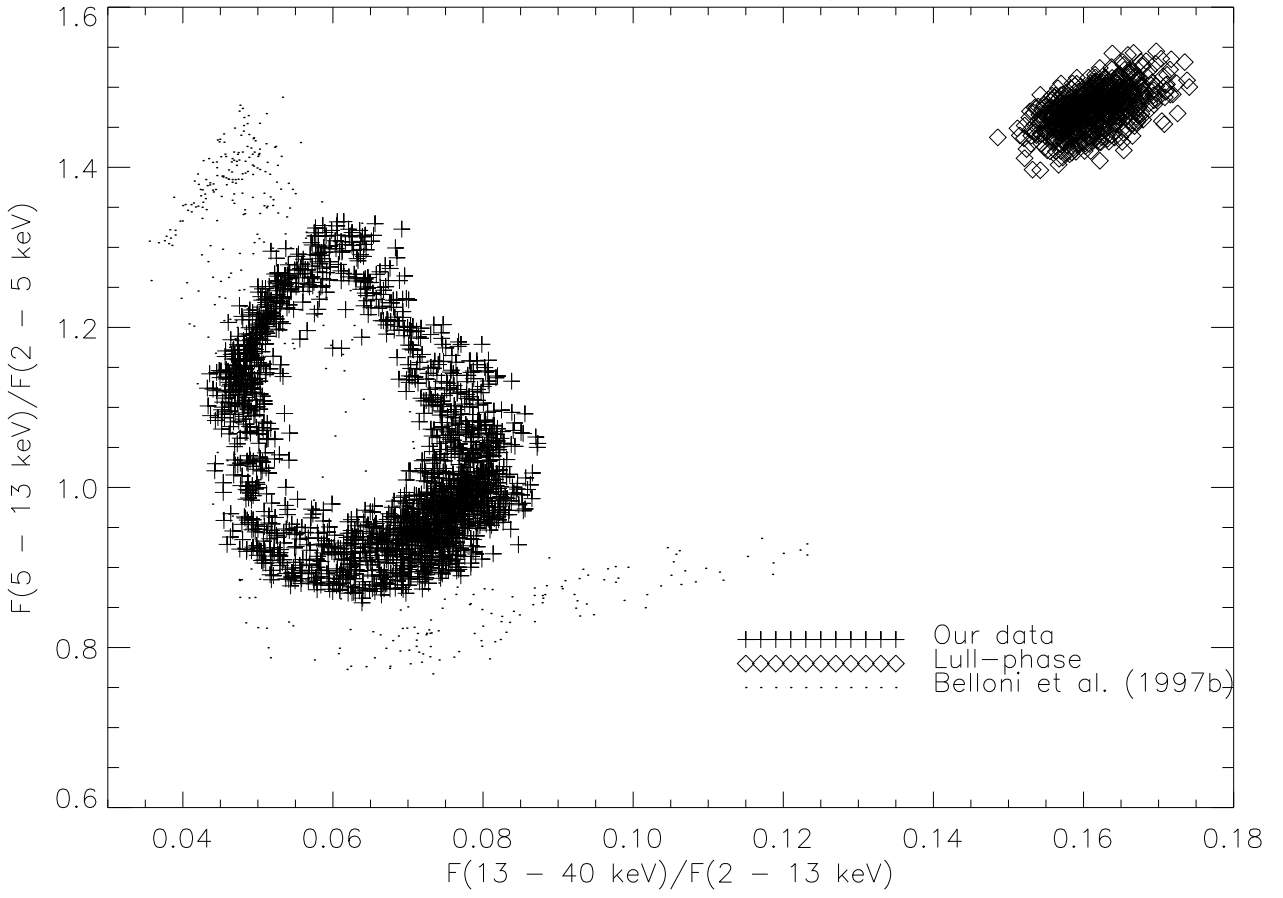
Fig. 4.— Selected light curves for the observation 20402-01-30-00 (from Fig.3): the total count rate 2 - 40 keV (5 PCU's, in units of 15000 cts/s), the inner disk temperature T_{in} , the Thomson optical depth τ multiplied by the electron temperature T_e of the spherical corona ($\tau T_e/50\text{keV}$) and the inner disk radius R_{in} .

Fig. 5.— Mean light curves over one cycle for the observation of Fig.3. The parameters are scaled by the following values (in parentheses): RATE (15000 cts/s (5 PCU units), solid line), R_{in} (35 km, dotted line), τ_{50} (1.4, dashed line) and \dot{M} ($0.75L_{Edd}/c^2$ of $10M_{\odot}$, dash-dotted line). Two identical cycles are plotted for clarity.

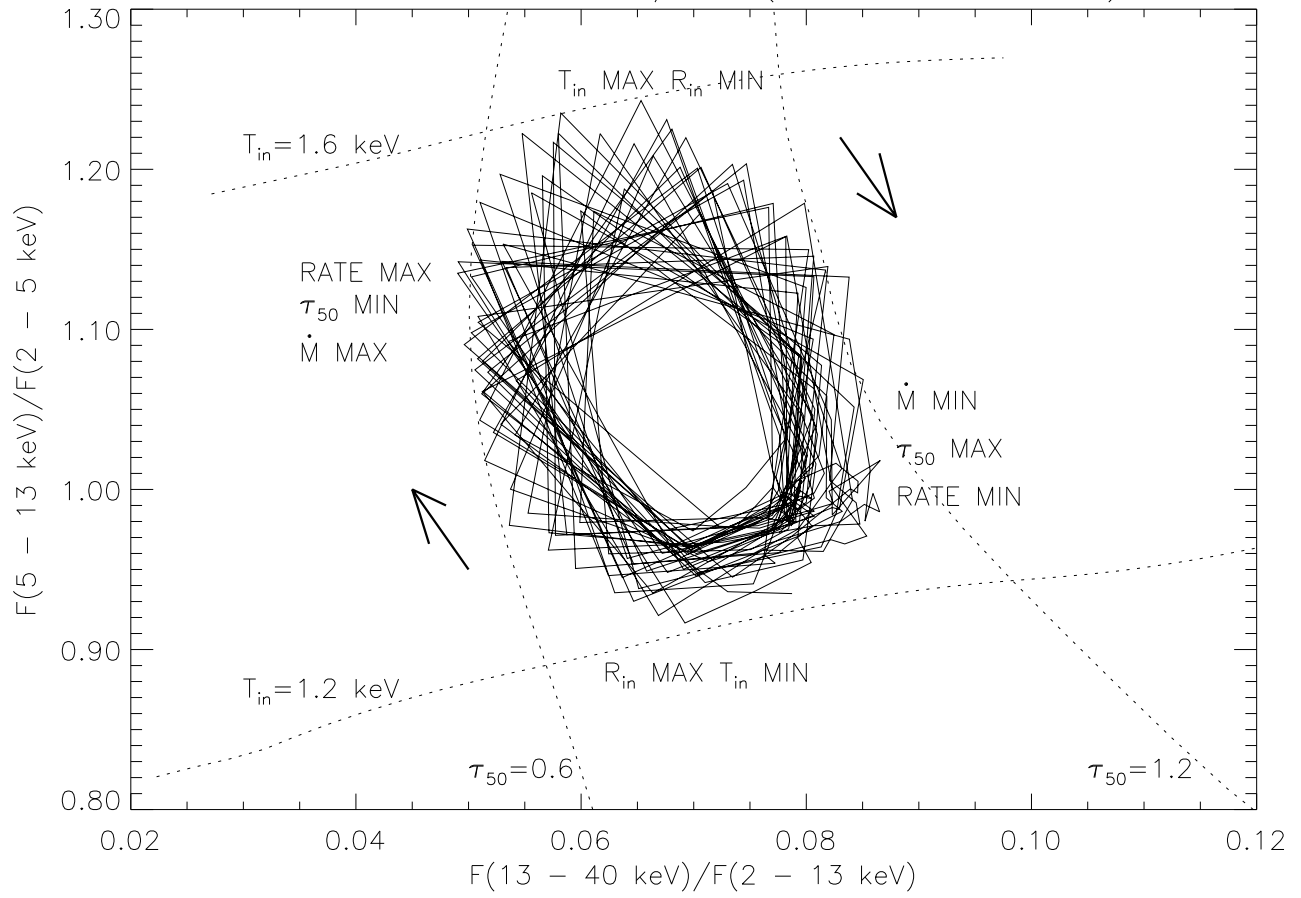
GRS 1915+105 RXTE/ASM



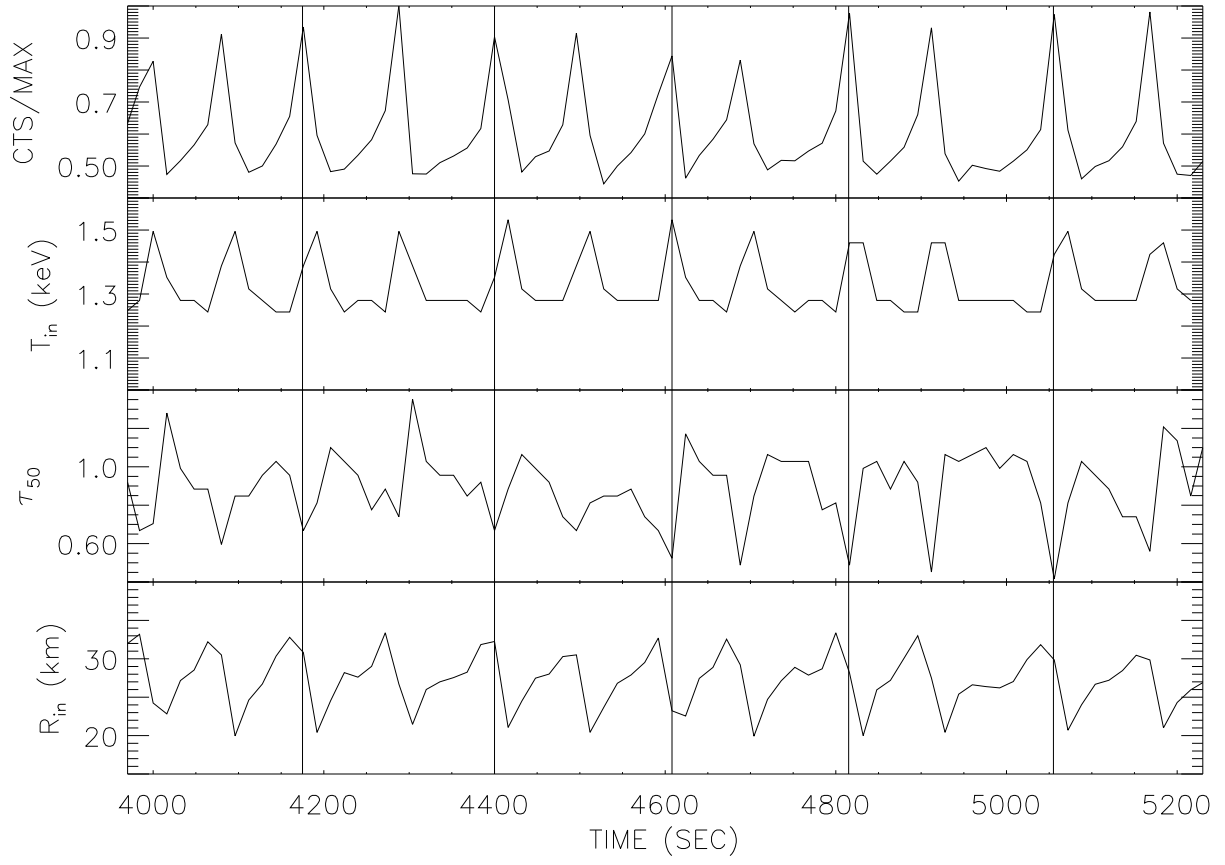
GRS 1915+105 RXTE/PCA



GRS 1915+105 RXTE/PCA (20402-01-30-00)



GRS 1915+105 RXTE/PCA



GRS 1915+105 RXTE/PCA MEAN LIGHT CURVES (20402-01-30-00)

